LC-DET-2002-011
October 2002

The MeV Gamma Compton Polarimeter for the SLAC FFTB Undulator Test

Vahagn Gharibyan[1,2], K. Peter Schüler[1]

[1]DESY, Deutsches Elektronen Synchrotron, Hamburg, Germany
[2]Yerevan Physics Institute, Yerevan, Armenia

Abstract

This note describes a Compton polarimeter for the FFTB undulator photon beam experiment at SLAC. Photons of a few MeV are scattered off polarized electrons in a thin ferromagnetic foil target. Photons are detected with a simple calorimetric detector which is mounted under a fixed scattering angle behind a small collimator aperture. We have evaluated the expected performance of the device as a function of undulator collimation angle and of the Compton scattering angle.

Contents

1 Introduction and Overview

A full exploitation of the physics potential of future linear colliders such as NLC and TESLA will require the development of polarized positron beams. In the proposed scheme of Balakin and Mikhailichenkov [1] a helical undulator is employed to generate photons of several MeV with circular polarization which are then converted in a relatively thin titanium target to generate longitudinally polarized positrons [2].

In order to test and develop this concept, it is being proposed [3] to employ a short test undulator [4] in the FFTB 50 GeV beam line at SLAC. For the first stage of this experiment it is planned to evaluate the flux and the spectrum of the undulator photons and to measure their degree of circular polarization. Two different gamma polarimeters are envisaged for this test.

A transmission type Compton polarimeter as first used by Goldhaber et al. [5] employs a thick magnetized iron target in the photon beam. A similar device was recently operated in tests at ATF in Japan [6].

In this note we describe a scattering type of Compton polarimeter which employs a thin ferromagnetic foil target in the photon beam. Arichev, Potylitsyn, and Strikanov [7] have proposed a polarimeter of this type for tests at KEK-ATF. In their study they proposed to detect the recoil Compton electrons. In our study we came, however, to the conclusion that it is vital to detect the scattered photons instead.

The reason is that multiple scattering of low energy electrons ($\sim 5\ MeV$) is so large, even in very thin target foils, as to essentially destroy the kinematic information of interest. Fortunately this problem can be avoided if we detect the scattered photons instead. Furthermore we can eliminate the pair-production background that would be significant in the case of electron detection, by use of a simple sweeping magnet.

The experimental layout of the scattering polarimeter that will be investigated in this note is quite simple and shown in Fig.1. The undulator beam is collimated by a small aperture C_1 before it strikes the iron foil target (Tgt). The electron polarization of the target can be flipped by reversing a modest external field that is generated by a pair of Helmholtz coils (H). A calorimetric detector (Det) is mounted behind apertures C_2 and C_3 which define a fixed scattering angle. A small sweeping magnet removes any charged component from the scattered photon beam axis.

In chapter 2 of this note we will review some basic kinematic features, as well as the cross sections and spin asymmetries of the Compton process. In chapter 3 we describe the undulator photon spectrum, its angular distribution and polarization behavior. In chapter 4 we will concoct this into observable detector signals and spin asymmetries. Chapter 5 gives further information about the experimental configuration. In chapter 6 we give results of Monte Carlo event simulations, event rates and statistical errors of the polarization measurement. Chapter 7 gives a conclusion.

2 Kinematics, Cross Sections, Spin Asymmetry

We review briefly some of the basic features of the Compton scattering process.

Definitions:

ω_0 and ω are the initial and final photon energies;
$E_0 = mc^2$ and E are the initial and final energies of the recoil electron;
θ and θ_e are the scattering angles of the photon and the electron.

The energies of are related through energy conservation

$$\omega_0 \ + \ mc^2 \ = \ \omega \ + \ E \tag{1}$$

Furthermore, from momentum conservation follows

$$\omega \ = \ \frac{\omega_0}{1 \ + \ (\omega_0/mc^2)\,(1 - cos\ \theta)} \tag{2}$$

The scattered photon and the scattered electron angles relative to the photon beam direction are

$$cos\ \theta \ = \ 1 \ - \ \frac{mc^2}{\omega_0}\left(\frac{\omega_0}{\omega} \ - \ 1\right) \tag{3}$$

$$tg(\theta_e) \ = \ \frac{ctg(\theta/2)}{1 + \omega/mc^2} \tag{4}$$

The spin-dependent differential Compton cross section is

$$\frac{d\sigma}{d\Omega} \ = \ \frac{d\sigma_0}{d\Omega}\ (1 + P_\gamma P_e A) \tag{5}$$

with the unpolarized part

$$\frac{d\sigma_0}{d\Omega} = \frac{{r_0}^2}{2}\left(\frac{\omega}{\omega_0}\right)^2\left(\frac{\omega_0}{\omega} + \frac{\omega}{\omega_0} - sin^2\,\theta\right) \tag{6}$$

where r_0 is the classical electron radius and

$$\frac{r_0^2}{2} = 39.71\ mb \tag{7}$$

and P_γ and P_e are the longitudinal polarizations or helicities of the initial beam photon and the target electron.

The spin asymmetry is given by

$$A = \frac{d\sigma_{1/2} - d\sigma_{3/2}}{d\sigma_{1/2} + d\sigma_{3/2}} = \frac{(\omega_0/\omega\ -\ \omega/\omega_0)\ cos\ \theta}{\omega_0/\omega\ +\ \omega/\omega_0\ -\ sin^2\ \theta} \tag{8}$$

The energy spectra of the scattered photon and electron are mirror images of each other because of equation 1. The spectra are continuous and extend from a minimum photon energy ω_{min} for backward scattering ($\theta = 180^o$)

$$\omega_{min} = \frac{mc^2}{2\ +\ mc^2/\omega_0} \tag{9}$$

all the way up to the beam energy ω_0 for forward scattering ($\theta = 0$).

In Fig. 2a,b we give for a monochromatic beam energy of 5 MeV and 9.6 MeV the differential cross sections $d\sigma/d\Omega$ in mbarn/sterad as a function of the the photon scattering angle θ for $P_\gamma P_e\ =\ +1,\ -1,\ and\ 0$; furthermore the spin asymmetry A and the figure of merit $A^2 d\sigma/d\Omega$. The same quantities are shown in Fig. 3a,b as a function of the scattered photon and electron energies.

3 Undulator Spectrum

For the purpose of this polarimeter study, we need to know the energy spectrum and polarization behavior of the undulator photons.

The following undulator parameters have been assumed

electron beam energy	50 GeV
magnetic field	0.760 T
undulator period	2.4 mm
K value	0.1704
length of undulator	1 m
M (no. of periods)	417

The first harmonic of the undulator spectrum is given by

$$\frac{dN_\gamma}{ds} \;=\; 4\pi\alpha\, M\, \frac{K^2}{1+K^2} \cdot \frac{1}{2}\,(1-2s+2s^2) \tag{10}$$

where $s \;=\; \omega_0/\omega_0^{max}$ is the reduced energy variable, $\omega_0^{max} \;=\; 9.613\; MeV$, and $\alpha \;=\; 1/137$.

Numerically we have then

$$\frac{dN_\gamma}{ds} \;=\; 1.078 \cdot \frac{1}{2}\,(1-2s+2s^2) \tag{11}$$

with the total number of undulator photons (per 50 GeV electron) given by

$$N_\gamma \;=\; \int_0^1 \frac{dN_\gamma}{ds} ds \;=\; 0.359 \tag{12}$$

The relation between the emission angle θ and the energy variable s is

$$s \;=\; \frac{1}{1+\gamma^2\theta^2/(1+K^2)} \tag{13}$$

or

$$\theta \;=\; \frac{1}{\gamma}\sqrt{(1+K^2)\,(1-s)/s} \tag{14}$$

with $\gamma \;=\; 50\; GeV\; /mc^2 \;=\; 10^5$.

The circular polarization of the undulator radiation is given by

$$P_\gamma \;=\; \frac{2s-1}{1-2s+2s^2} \tag{15}$$

We have plotted these distributions in Fig. 4. Contributions from higher harmonics may be neglected.

4 Detector Signals and Asymmetries

We shall assume that we will detect Compton scattered photons behind a suitable collimator aperture (designated C_2 in Fig. 1) which subtends a solid angle $d\Omega$ at a fixed scattering angle θ. If the photon beam would be monochromatic, the detector would then be illuminated with photons of a fixed energy $\omega \;=\; f(\theta, \omega_0)$, with the function given by Equation (2).

Actually, however, the undulator photons are not at all monochromatic, but cover a broad spectrum of parabolic shape that reaches from zero to $\omega_0^{max} \;=\; 9.613\; MeV$ as shown in Fig. 4. Furthermore, the circular polarization of these undulator photons changes from -1 to +1 over this energy range, with a zero crossing at the midpoint energy of 4.807 MeV.

As the detector will not be able to count individual photon events, it will record an analog signal which is the superposition of all the single photon signals as obtained after integration over the entire undulator spectrum $(dN_\gamma/d\omega_0)(\omega_0)$.

$$S \;=\; \sum s_i \;=\; d\Omega \int_{\omega_0^{min}}^{\omega_0^{max}} \frac{dN_\gamma}{d\omega_0}(\omega_0)\, \frac{d\sigma_0}{d\Omega}(\theta,\omega_0)\,[1 + P_e P_\gamma(\omega_0) A(\theta,\omega_0)]\, d\omega_0 \tag{16}$$

If the detected signal is not proportional to the number of photons, but instead to the sum of their energies (as would be obtained with a calorimetric detector), we have to integrate an energy weighted expression.

$$W \;=\; \sum w_i \;=\; d\Omega \int_{\omega_0^{min}}^{\omega_0^{max}} \frac{dN_\gamma}{d\omega_0}(\omega_0)\, \frac{d\sigma_0}{d\Omega}(\theta,\omega_0)\,[1 + P_e P_\gamma(\omega_0) A(\theta,\omega_0)]\, \omega(\theta,\omega_0)\, d\omega_0 \tag{17}$$

Please note that these expressions depend on the polarization of the electron target P_e. We can operate the target with positive (+) and with negative (-) polarization, where we assume equal magnitudes so that $P_e(+) = -P_e(-) = P_e$.

We can then form the following experimental signal asymmetry

$$A_S \;=\; \frac{1}{P_e}\frac{S_+ - S_-}{S_+ + S_-} \;=\; \frac{1}{S_0}\int P_\gamma(\omega_0) A(\theta,\omega_0)\, d\omega_0 \tag{18}$$

and similarly for the energy weighted signals

$$A_W \;=\; \frac{1}{P_e}\frac{W_+ - W_-}{W_+ + W_-} \;=\; \frac{1}{W_0}\int P_\gamma(\omega_0) A(\theta,\omega_0)\, \omega(\theta,\omega_0)\, d\omega_0 \tag{19}$$

where the normalizations S_0 and W_0 are just the unpolarized parts in equations (16) and (17).

$$S_0 \;=\; d\Omega \int \frac{dN_\gamma}{d\omega_0}(\omega_0)\, \frac{d\sigma_0}{d\Omega}(\theta,\omega_0)\, d\omega_0 \tag{20}$$

$$W_0 \;=\; d\Omega \int \frac{dN_\gamma}{d\omega_0}(\omega_0)\, \frac{d\sigma_0}{d\Omega}(\theta,\omega_0)\, \omega(\theta,\omega_0)\, d\omega_0 \tag{21}$$

We have evaluated the asymmetries A_W and A_S in Fig. 5a and Fig. 5b as a function of the scattering angle θ. The different curves shown correspond to different undulator collimation angles.

Undulator collimation will eliminate all beam photons below a corresponding threshold (see equ. 14) and will therefore control the lower integration limit ω_0^{min}. For example an undulator collimation of $10\,\mu rad$ would eliminate the lower half of the undulator spectrum with its undesirable negative polarization. The degree of undulator collimation that can be applied has a dramatic effect on the mean photon polarization and the observable polarimeter asymmetry.

Also shown are the spin-averaged signals S_0 and W_0 (labeled as $d\sigma/d\Omega$) and the statistical figures of merit $A_S^2 S_0$ and $A_W^2 W_0$ (labeled as $A^2 d\sigma/d\Omega$), corresponding to either unweighted or energy-weighted photon detection. Energy-weighted detection favors higher photon energies and thus slightly smaller scattering angles. A scattering angle of 17^o appears to be a reasonable compromise that would accommodate useful asymmetry measurements with both detection techniques for all possible collimation cases.

5 Experimental Configuration

We refer to Fig. 1 for a discussion of the experimental configuration.

The undulator photon beam enters from the left and is collimated by C_1. This collimator must be located at a considerable distance from the undulator in order to achieve the very small collimation angles that would be desirable. For example, a $10\,\mu rad$ collimation angle could be realized with an aperture diameter of $0.5\,mm$ at a distance of $25\,m$.

The collimated undulator beam strikes then the polarized electron target (Tgt) which consists of a thin ferromagnetic foil which is tilted by a shallow angle of 20^o against the beam direction. The foil is magnetized by a modest external field from a pair of Helmholtz coils (H) which may be reversed every few minutes. At saturation an electron polarization of about 8% is achieved.

Such a target has been employed in numerous Moller scattering experiments in end-station A at SLAC since 1975. That device could be used, if it still exists, but would need a somewhat larger exit flange to accommodate a scattering angle of $(17 \pm 1)^o$. Recently it has been demonstrated that Moller target foils can also be oriented square to the beam direction under certain conditions, but this requires very high external fields [8, 9].

Scattered photons are then detected by a single calorimeter channel which measures the integrated energy deposition per accelerator pulse. The scattering angle and the covered solid angle are fixed by the position and aperture of collimator C_2: $\theta = (17 \pm 1)^o$, $\Delta\phi = 2^o$, $\Delta\Omega = 3.56 \cdot 10^{-4}$.

Finally a small sweeping magnet (SM) with about 0.01 Tm would be sufficient to deflect any charged component out of the scattered photon beam path. This will remove recoil Compton electrons, but also pair production background.

6 Event Rates and Statistical Errors

In order to understand the response of the polarimeter as well as possible, we have generated Monte Carlo events which simulate the undulator spectrum and the Compton scattering process as described in the previous chapters.

For the simulation we used the following standard assumptions and parameters

Electron Beam	
energy	50 GeV
electrons per bunch	$1 \cdot 10^{10}$
bunches per second	30 Hz
Undulator	
photons per e^-	0.359
ω^{max}	9.613 MeV
spectrum	equ. 11, fig. 4
angular distribution	equ. 14, fig. 4
collimation angle	variable
polarization	equ. 15, fig. 4
Target	
material	Fe
thickness	100 μm
tilt angle	20^o
polarization	0.08
Spectrometer	
scattering angle θ	17^o
$\Delta\theta$	$\pm 1^o$
$\Delta\phi$	$\pm 1^o$
$\Delta\Omega$	$3.56 \cdot 10^{-4}$

The results of the simulations are shown in Fig. 6 for six different undulator collimations from $5\mu rad$ to $100\mu rad$. Two dimensional event distributions in scattered photon energy vs. angle are shown in the upper plot. The lower plot shows the detected photon event spectrum. For each of the six simulations we generated a total of $2 \cdot 10^9$ beam electrons and thus $0.72 \cdot 10^9$ undulator photons, equally divided between the two target polarization states.

The following table gives for each of the simulations the mean detected photon energy $\langle\omega\rangle$, the energy sum $\sum \omega/pulse$, the number of detected photons $\sum N/pulse$, where these numbers had to be scaled from the obtained Monte Carlo statistics, and finally the statistical error $\Delta P/P$ in the polarization measurement obtained in one minute of data taking.

collimation angle (μrad)	$\langle\omega\rangle$ (MeV)	$\sum\omega/pulse$ (GeV)	$\sum N/pulse$	$\Delta P/P$ per min. (%)
5	5.1	7.69	1570	1.2
10	4.6	16.82	3848	1.1
15	4.0	22.49	5847	1.5
30	3.1	28.17	9602	1.9
50	2.8	28.88	11081	1.8
100	2.7	28.92	11502	1.8

In order to avoid misunderstandings we want to emphasize that the high photon statistics materializes in the form of an analog signal during the very short bunch length, i.e. these photons can not actually be counted. Nevertheless, we may use these simulated numbers to calculate statistical errors. We conclude that errors based on event statistics will be exceedingly small in comparison with systematic effects.

We will not attempt a discussion of systematic errors in this paper, except to state that we expect an overall systematic uncertainty of the order of 3% as typical for standard Moller target experiments.

7 Summary and Conclusion

We have presented a design of a scattering type Compton polarimeter for the measurement of circular polarization of very high intensity undulator photons. The experimental configuration is quite simple and can be quickly implemented from existing components. The precision of the polarization measurement is expected to be determined by systematic errors at the level of 3%.

8 Acknowledgements

We thank our colleague Klaus Flöttmann for providing us with the essential undulator data. This work was greatly stimulated by lively discussions with Rainer Pitthan, John Sheppard, Norbert Meyners and Gudrid Moortgat-Pick. Finally we like to thank Rolf-Dieter Heuer and Robert Klanner for their support and encouragement.

References

[1] V.E. Balakin and A.A. Mikhaillichenko, *The Conversion System for Obtaining High Polarized Electrons and Positrons*, Preprint INP 79-85, 1979.

[2] K. Flöttmann, *Investigation Toward the Development of Polarized and Unpolarized High Intensity Positron Sources for Linear Colliders*, DESY-93-161, 1993.

[3] K. McDonald and collaborators, *A 2-Stage Proposal to Test Production of Polarized Positrons with the SLAC 50 GeV Beam in the FFTB*, SLAC-Proposal-E16x, October 20, 2002.

[4] Alexander A. Mikhailichenko, *Pulsed Helical Undulator for Test at SLAC of the Polarized Positron Production Scheme*, Cornell Note CBN 02-10, September 2002.

[5] M. Goldhaber, L. Grodzins, and A.W. Sunyar, *Evidence for Circular Polarization of Bremsstrahlung Produced by Beta Rays*, Phys. Rev. 106 (1957) 826.

[6] M. Fukuda, T. Hirose, I. Sakai, T. Aoki, M. Washio, T. Iimura, Y. Kurihara, T. Okugi, T. Omori, J. Urakawa, *Polarimetry of Short Pulse Gamma-Rays and Positrons*, Proc. of the Second Asian Particle Accelerator Conference, Beijing, China, 2001;
I. Sakai, T. Hirose, K. Dobashi, M. Fukuda, Y. Kamiya, M. Washio, A. Higurashi, T. Oshima, T. Aoki, J. Urakawa, T. Okugi, Y. Kurihara, T. Omori, *Polarized Positron Experiment at ATF*, talk.

[7] A.S. Arychev, A.P. Potylitsyn, M.N. Strikhanov, *Determination of Circular Polarization of γ-Quanta With Energy ¿ 10 MeV Using Compton Polarimeter*, arxiv.org/pdf/physics/0112060; arxiv.org/list/physics/0112-70k.

[8] L.V. de Bever, J. Jourdan, M. Loppacher, S. Robinson, I. Sick, J. Zhao, *A target for precise Møller polarimetry*, Nucl. Instr. Meth. A400 (1997) 379.

[9] M. Hauger, A. Honegger, J. Jourdan, G. Kubon, T. Petitjean, D. Rohe, I. Sick, G. Warren, H. Wöhrle, J. Zhao, R. Ent, J. Mitchell, D. Crabb, A. Tobias, M. Zeier, B. Zihlmann, *A High-Precision Polarimeter*, Submitted to Nucl. Instr. Meth., e-print archive: nucl-ex/9910013.

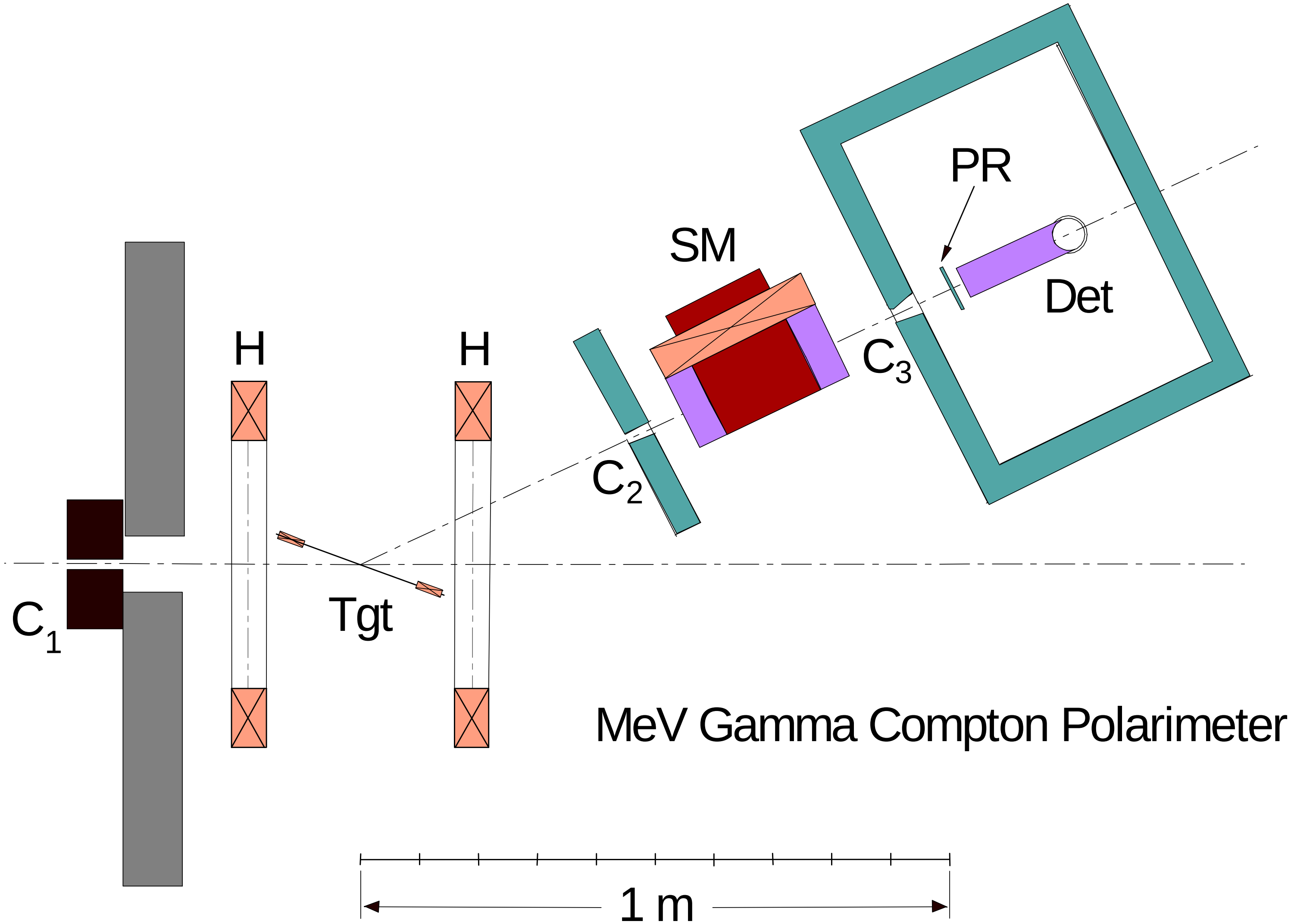

Figure 1: Experimental Layout

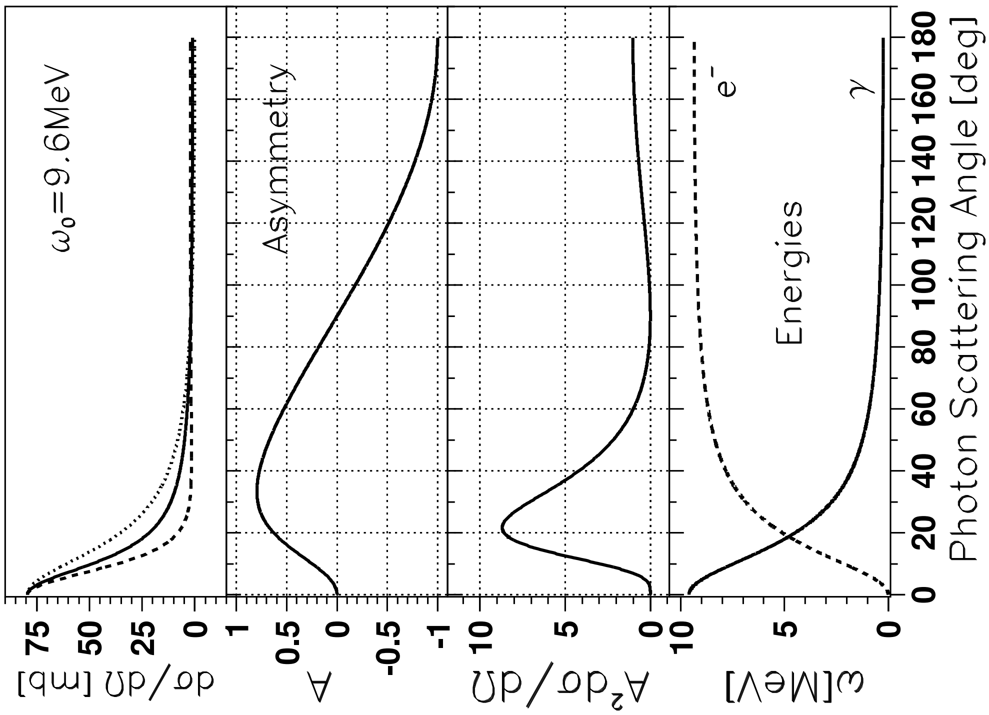

Figure 2: b Distributions vs. Angle (9.6 MeV monochr. beam)

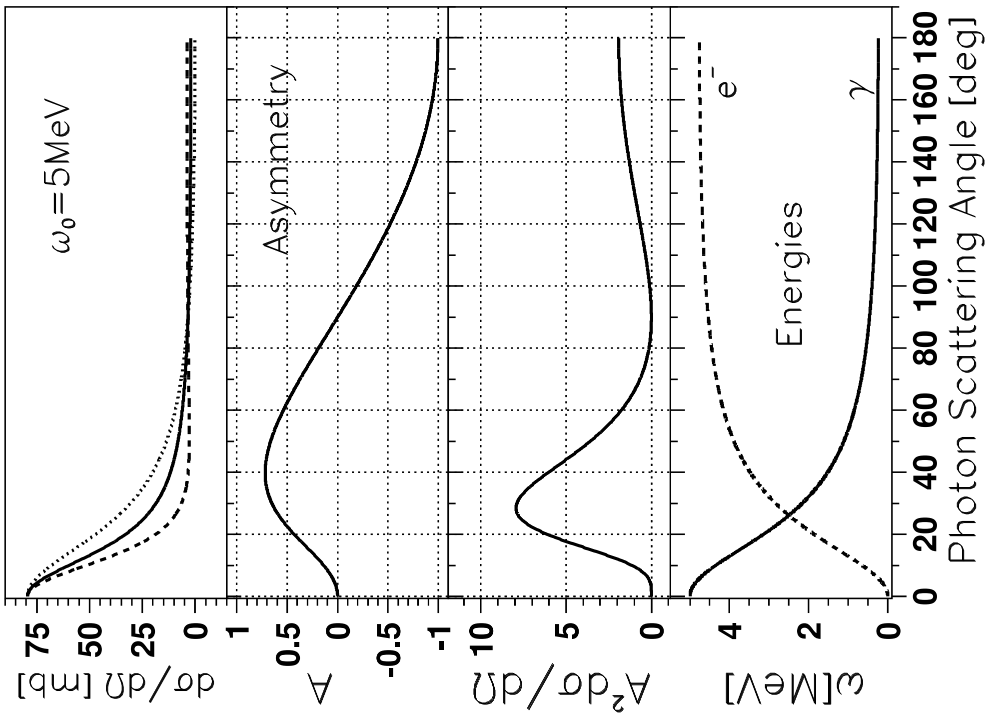

Figure 2: a Distributions vs. Angle (5 MeV monochr. beam)

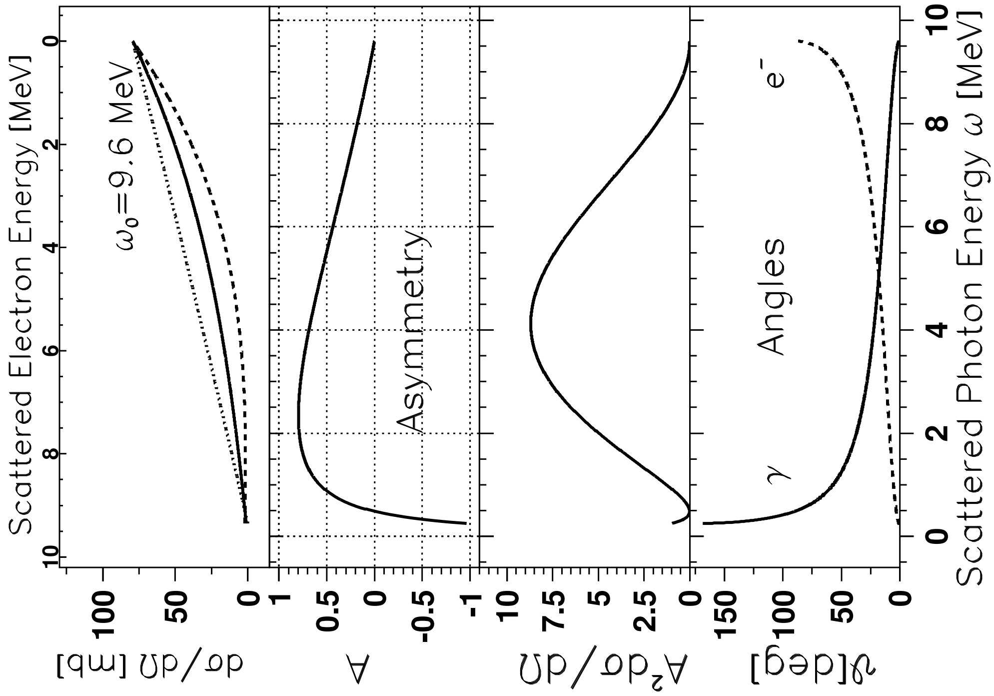

Figure 3: b Distributions vs. Energy (9.6 MeV monochr. beam)

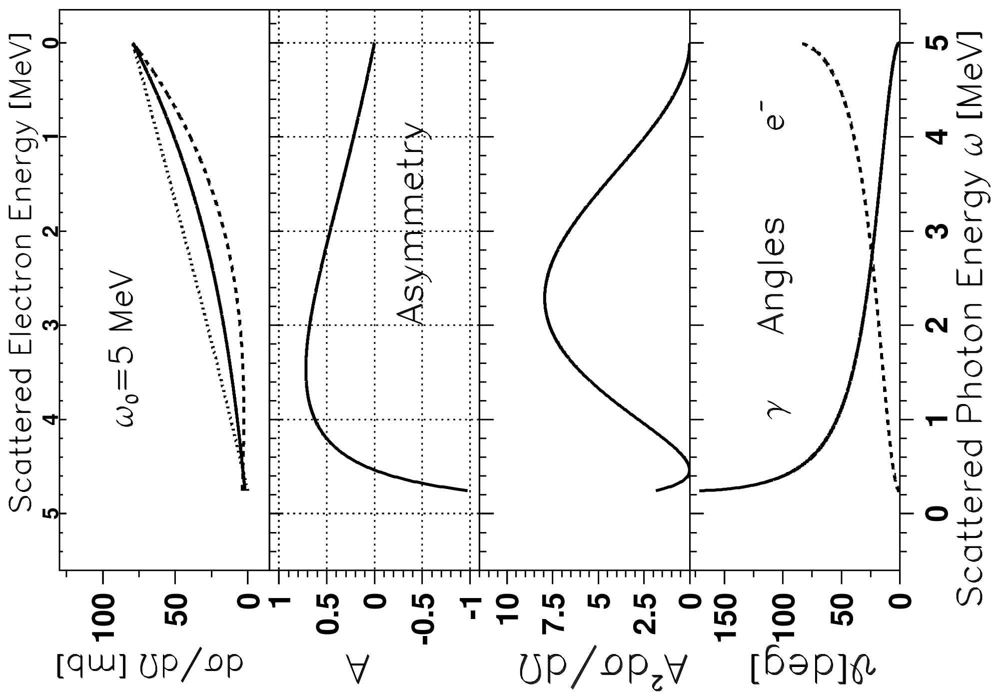

Figure 3: a Distributions vs. Energy (5 MeV monochr. beam)

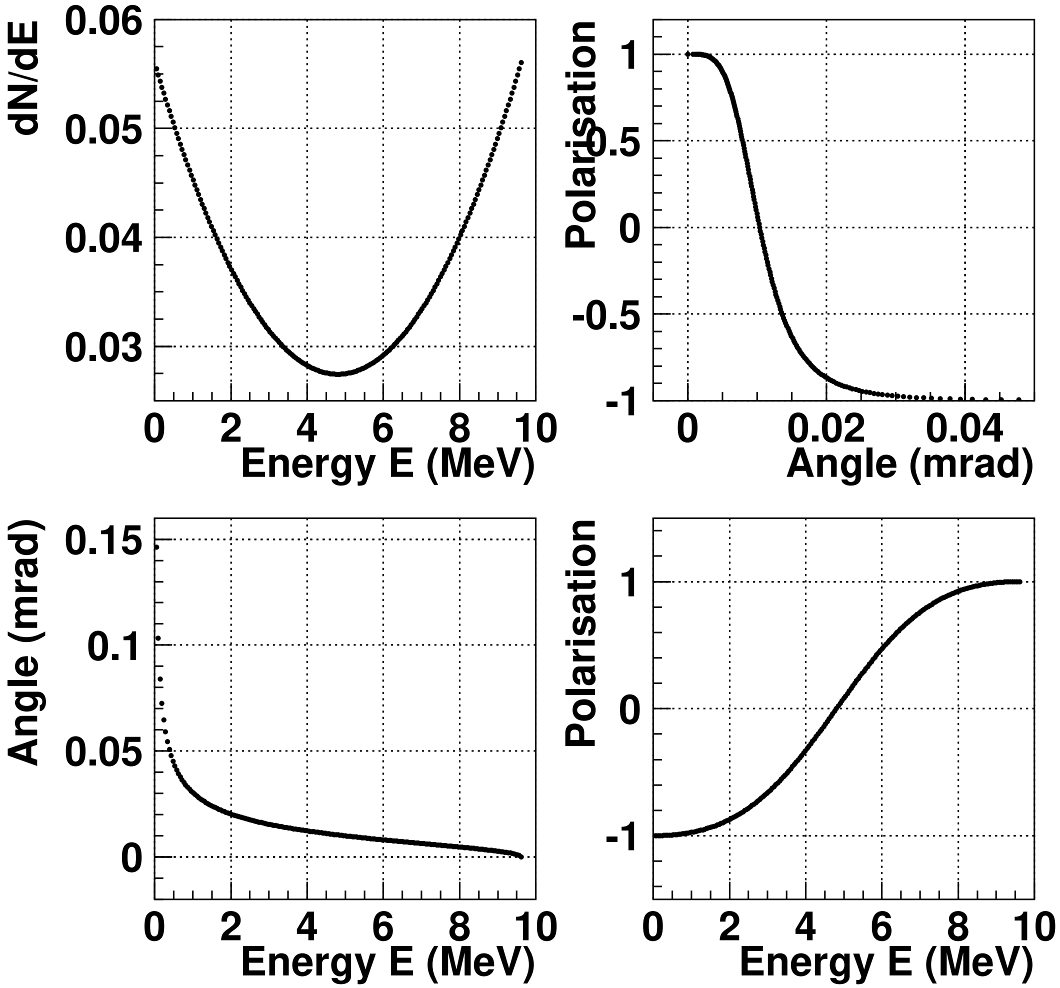

Figure 4: Undulator Spectrum, Polarization and Angular Distribution

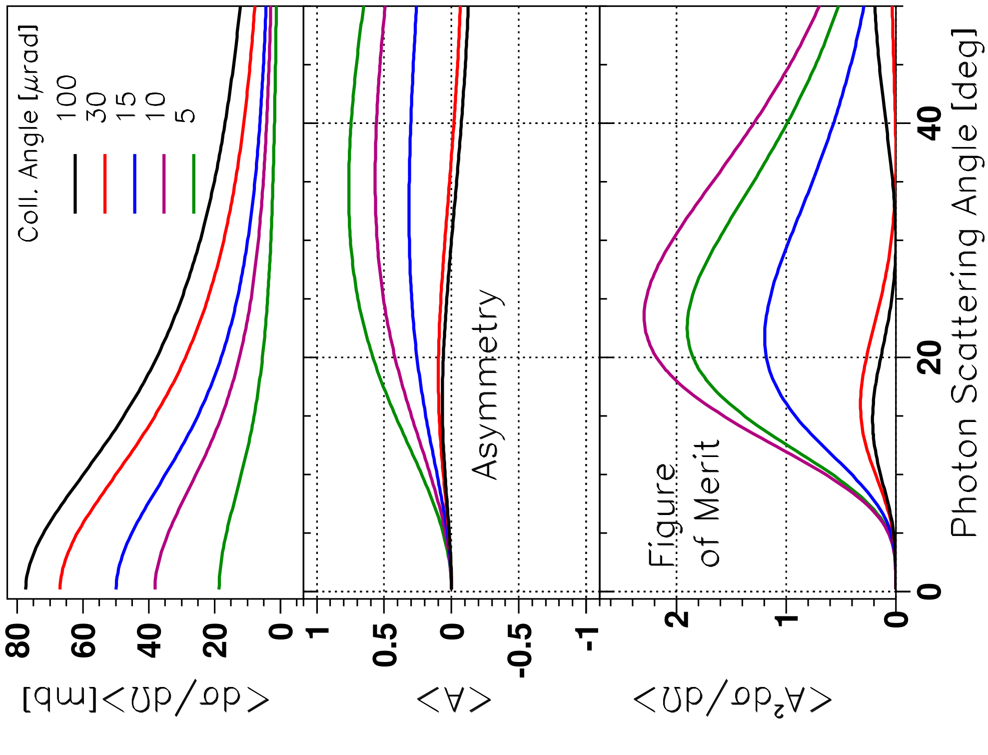

Figure 5: b Integrated Count Signals

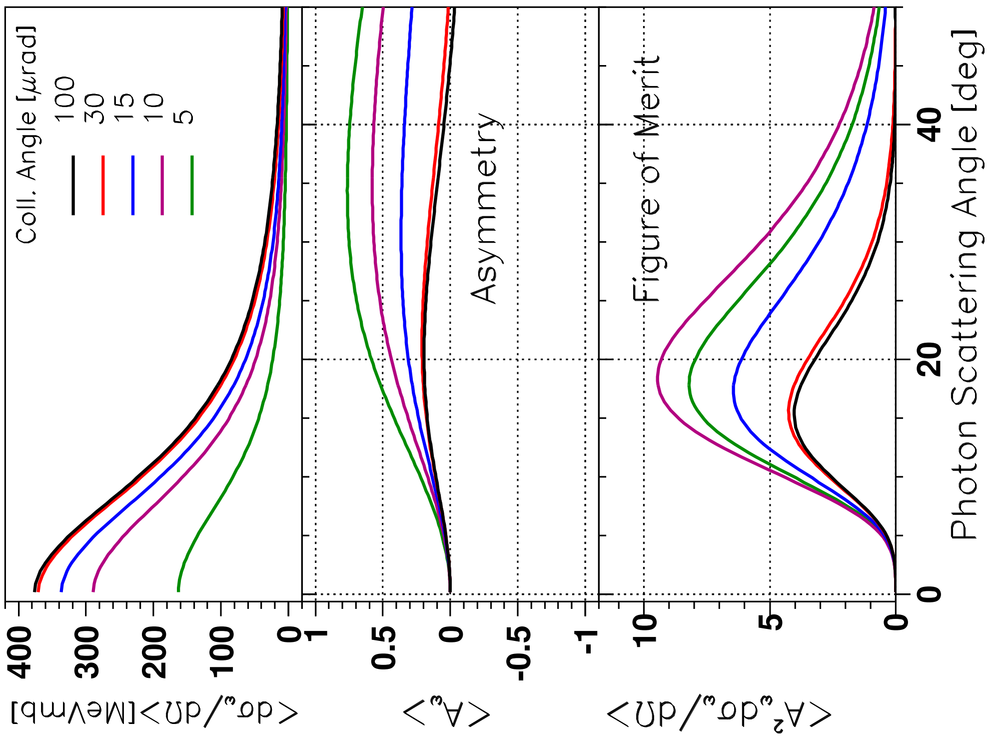

Figure 5: a Integrated Energy Signals

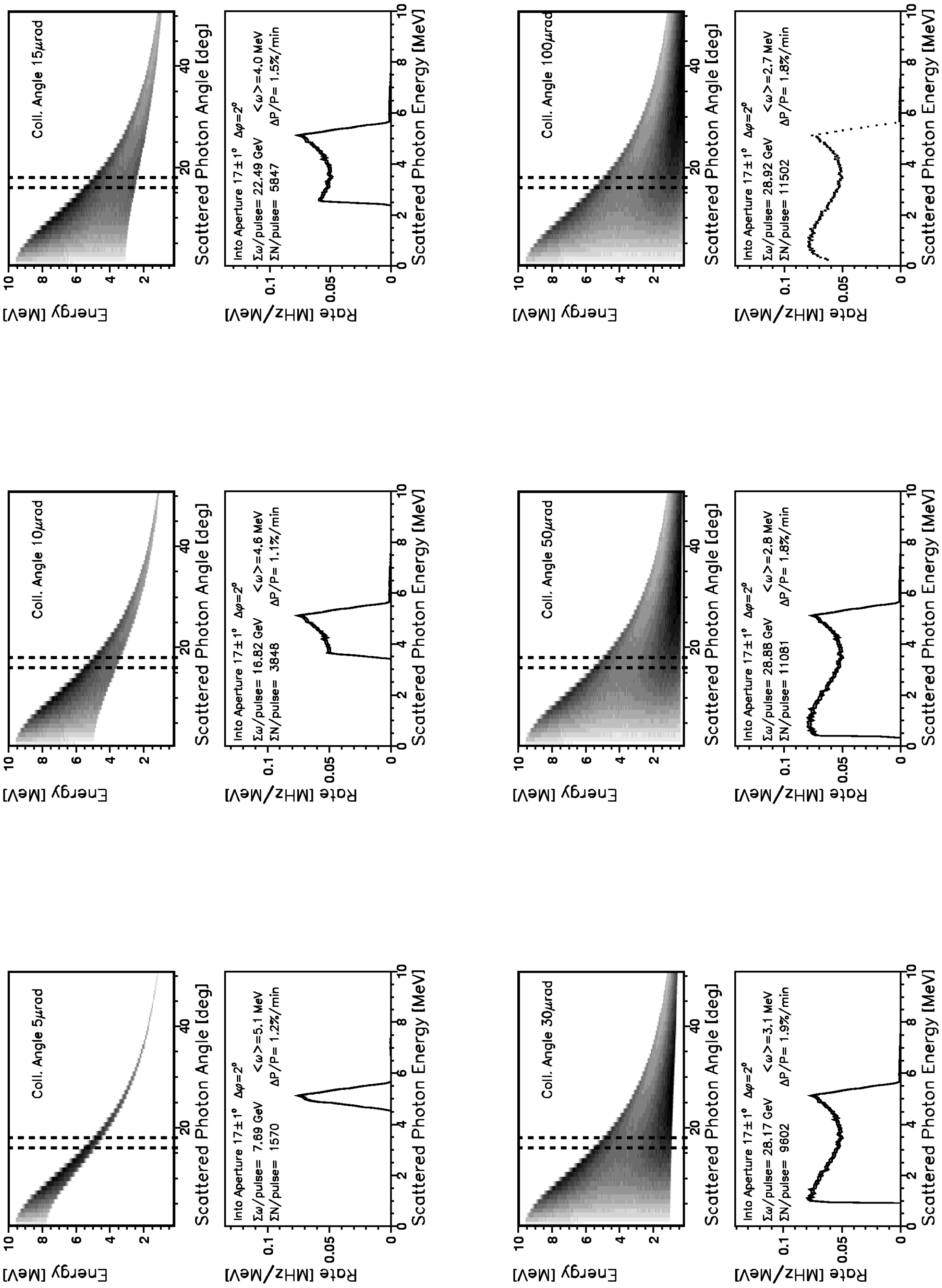

Figure 6: Monte Carlo Results